Chemometrics and Intelligent Laboratory Systems 177 (2018) 83–88

Contents lists available at ScienceDirect

Chemometrics and Intelligent Laboratory Systems

journal homepage: www.elsevier.com/locate/chemometrics

Discrete Hermite moments and their application in chemometrics

Barmak Honarvar Shakibaei Asli [a,*], Jan Flusser [a,b]

[a] Institute of Information Theory and Automation, Academy of Sciences of the Czech Republic, Pod Vodárenskou Věží 4, 182 08 Praha 8, Czech Republic
[b] Faculty of Management, University of Economics, Jindřichuv Hradec, Czech Republic

ARTICLE INFO

Keywords:
Orthogonal polynomials
Discrete polynomials
Tchebichef moment
Hermite moment
Gauss–Hermite quadrature

ABSTRACT

In this paper, we provide comments on the recent paper by Bao Qiong Li et al. [1] that proposed a novel tool for chemometric analysis of three-dimensional spectra using Tchebichef–Hermite image moment method. We show that the proposed combined moments are not stable since the Tchebichef polynomials have a discrete instinct and Hermite polynomials are continuous. We use Gauss–Hermite quadrature to discretize continuous Hermite polynomials. A correct use of the discrete Hermite moments (DHMs) for numerical experiments is presented.

1. Introduction

The paper [1], that appeared in the May 2017 issue of this journal, introduced a new kind of image moments called Tchebichef–Hermite moments (THMs)[1] and proposed their usage in image analysis. The authors of [1] pointed out that the THM method not only inherits common advantages of these discrete orthogonal moments to deal with some fundamental challenges during the analytical process of different kinds of 3D spectra, but also has its unique superiority in information extraction ability that simplify the determination of optimum maximal orders in moment methods.

However, the above statement is highly misleading. In Ref. [1], two very important points are mentioned mistakenly. First, the THMs are actually not discrete orthogonal moments. Moreover, the proposed formulation is so unstable. Here, "stability" means the limitation of the dynamic range of the computed moments which exhibits a convergence behaviour when trying to reconstruct the signal from its moments. The method [1] is based on Tchebichef moments, that were introduced to image analysis community by Mukundan [2] and the well-known Hermite polynomials, which are also popular but which are orthogonal in a continuous domain [3,4]. The authors of [1] merged a discrete orthogonal polynomial with a continuous orthogonal polynomial to find a new discrete orthogonal moment. This is incorrect and does not make sense for digital images, because any orthogonal polynomial must be discretized to act as an image feature generator.

The aim of this paper is to distinguish between the continuous and discrete polynomials with respect to their orthogonality and, consequently, to show how the discretization of orthogonal Hermite polynomials can be performed correctly. We believe this could be helpful for the readers who want to use the method proposed in Ref. [1].

2. Discretization of Hermite polynomials

Classical continuous Hermite polynomials $H_n(x)$ are orthogonal on $(-\infty, +\infty)$ with respect to weight function $w(x) = e^{-x^2}$ as

$$\int_{-\infty}^{+\infty} H_n(x) H_m(x) e^{-x^2} \mathrm{d}x = 2^n n! \sqrt{\pi} \delta_{nm}, \tag{1}$$

where δ_{nm} is the Kronecker delta. As the authors of [1] correctly pointed out, Hermite polynomials are not orthonormal. To make them orthonormal, the normalization proposed in Ref. [4] can be applied

$$\overline{H}_n(x) = \frac{H_n(x)}{\sqrt{2^n n! \sqrt{\pi}}}. \tag{2}$$

To discretize these continuous polynomials, we use Gauss–Hermite quadrature which is an approximation of the definite integral of a function, usually stated as a weighted sum of function values at specified points within the domain of integration. In this case

* Corresponding author.
E-mail addresses: honarvar@utia.cas.cz (B.H. Shakibaei Asli), flusser@utia.cas.cz (J. Flusser).

[1] English spelling of the surname of that Russian mathematician should be Chebyshev rather than Tchebichef. The latter form comes from the French transcription. In this paper, we keep the form Tchebichef, which was used in Ref. [1], for the sake of consistency.

https://doi.org/10.1016/j.chemolab.2018.04.011
Received 15 January 2018; Received in revised form 8 April 2018; Accepted 12 April 2018
Available online 18 April 2018

$$\int_{-\infty}^{+\infty} f(x)e^{-x^2}\mathrm{d}x \approx \sum_{j=0}^{N-1} w_j f(x_j), \tag{3}$$

where N is the number of sample points used. The x_j are roots of Hermite polynomial $H_n(x)$, and the associated weights w_j are defined as

$$w_j = \frac{2^{N-1}N!\sqrt{\pi}}{N^2\left[H_{N-1}(x_j)\right]^2}.$$

Using the Gauss–Hermite quadrature rule converts the continuous orthogonality of Hermite polynomials to a discrete orthogonality as

$$\sum_{j=0}^{N-1} H_n(x_j)H_m(x_j)w(x_j, N) = \rho(n, N)\delta_{nm}. \tag{4}$$

where w and ρ are the weight and norm functions

$$w(x_j, N) = \frac{1}{\left[H_{N-1}(x_j)\right]^2} \quad ; \quad \rho(n, N) = \frac{2^{n-N+1}n!N^2}{N!}. \tag{5}$$

Eq. (4) expresses the discrete weighted orthogonality of Hermite polynomials. To achieve discrete orthonormality, we introduce weighted discrete Hermite polynomials defined by

$$\tilde{H}_n(x_j) = H_n(x_j)\sqrt{\frac{w(x_j, N)}{\rho(n, N)}}. \tag{6}$$

Eq. (4) then becomes

$$\sum_{j=0}^{N-1} \tilde{H}_n(x_j)\tilde{H}_m(x_j) = \delta_{nm}. \tag{7}$$

The graphs of the normalized continuous and weighted discrete Hermite polynomials are shown in Fig. 1. The upper graphs illustrate the low-order Hermite polynomials up to degree four. The curves at the bottom show the high-order Hermite polynomials from degree 45 to 49. In both cases of the discrete Hermite polynomials which are shown in Fig. 1(b) and (d), the number of sample points was 50. It can be seen from the graphs that the number of roots of the low order normalized continuous Hermite polynomials are the same as the number of roots of the high order weighted discrete Hermite polynomials. For example, both $\overline{H}_4(x)$ and $\tilde{H}_{45}(x_j)$ have four roots.

3. Discrete–Hermite moments (DHMs) vs. Tchebichef–Hermite moments (THMs)

As we mentioned in the introduction, the proposed THMs in Ref. [1] are not correct. The authors of that reference claimed that the THMs are in the category of discrete orthogonal moments which is not true. They also tried to combine the advantages of the Tchebichef and the Hermite moments but in their formulation, they only used the Hermite polynomials in continuous form in both dimensions (from the text and the terminology of [1], according to a widely-accepted nomenclature of moments, the reader would expect a combination of Hermite polynomials in one dimension and Tchebichef polynomials in the other one) with the normalized factor of the Tchebichef polynomials $\tilde{\rho}(n, N)$ (see Eqs. (5) and (6) of [1]). There is no mathematical justification of this approach and it is not clear what the authors believe is the benefit of that. Here, we show the correct form of the Hermite moments in discrete domain instead of their simple continuous forms. Since there is no combination between Tchebichef and Hermite moments in Ref. [1], we propose the discrete–Hermite moments (DHMs) as a new basis for 1D/2D signals analysis.

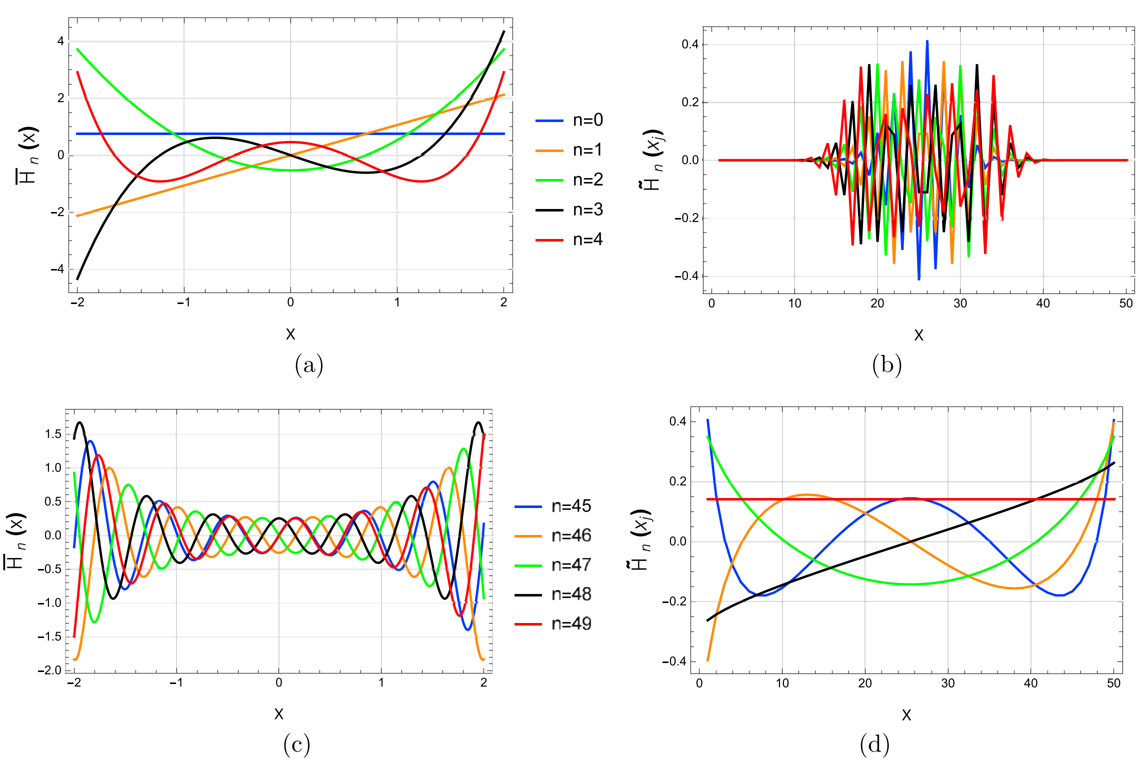

Fig. 1. Comparison between the discrete continuous Hermite polynomials for low and high orders: (a) normalized continuous Hermite polynomials up to 4^{th} order, (b) weighted discrete Hermite polynomials up to 4^{th} order ($N = 50$), (c) normalized continuous Hermite polynomials from order 45 up to 49 and (d) weighted discrete Hermite polynomials from order 45 up to 49 ($N = 50$).

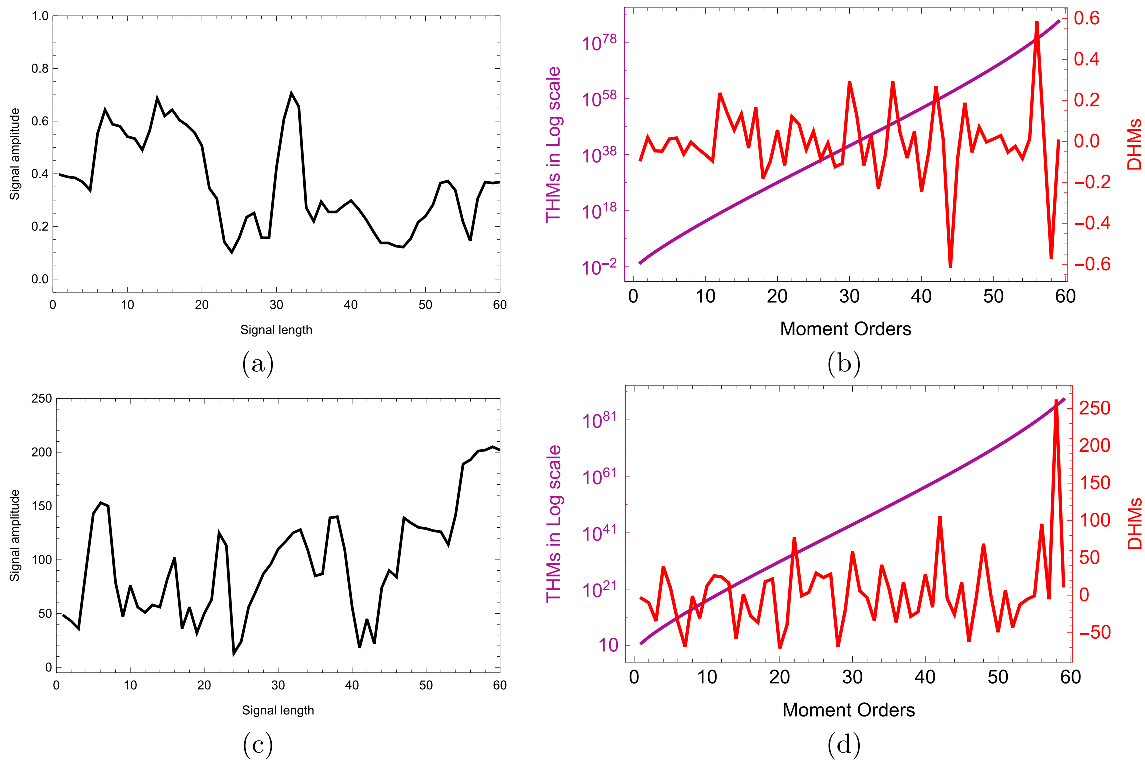

Fig. 2. Moment value distribution of a 1D signal with the length of 60 samples: (a) 1D signal quantized into $[0, 1]$, (b) THMs distribution in logarithmic scale (purple) and DHMs distribution (red) for the signal in (a), (c) 1D signal quantized into $[0, 255]$, (d) THMs distribution in logarithmic scale (purple) and DHMs distribution (red) for the signal in (c). (For interpretation of the references to colour in this figure legend, the reader is referred to the Web version of this article.)

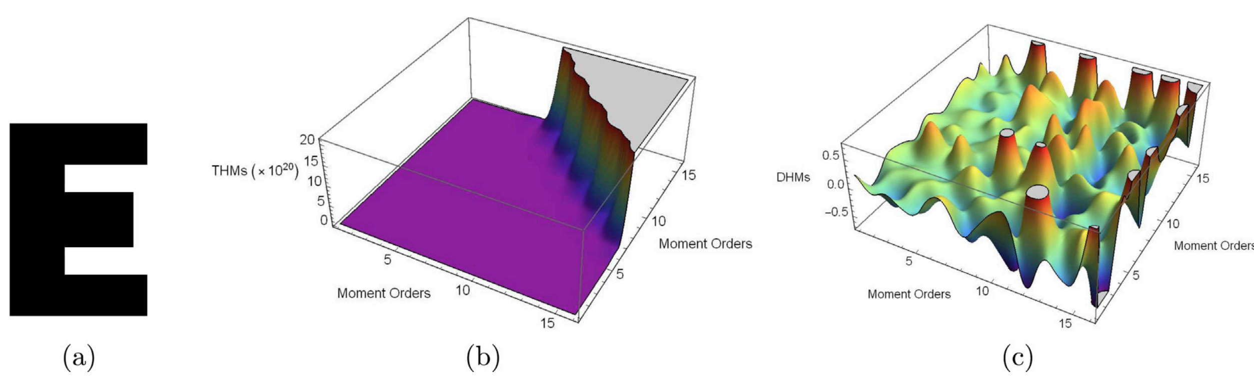

Fig. 3. Moment distribution of a 2D binary image: (a) the letter “E” of size 16×16, (b) THMs distribution, (c) DHMs distribution.

Thanks to their discrete orthogonality and even orthonormality (see Eq. (7)), discrete normalized Hermite polynomials $\tilde{H}_n(x_i)$ can be efficiently used in 2D signal/image analysis. We define DHMs as the "projections" of discrete signal f onto the set of discrete normalized Hermite polynomials. We can apply this approach in arbitrary dimensions. Particularly, in 2D we have

$$DHM_{n,m}(f) = \sum_{i=0}^{N-1} \sum_{j=0}^{M-1} \tilde{H}_n(x_i)\tilde{H}_m(x_j) f(i,j), \quad n = 0, 1, \ldots, N-1 \quad ; \quad m = 0, 1, \ldots, M-1. \tag{8}$$

DHMs may serve as the signal features/signatures. They provide a complete description of the signal, which means the original signal can be precisely reconstructed from them. Due to the orthogonality, the reconstruction is very simple since

$$f(i,j) = \sum_{n=0}^{N-1} \sum_{m=0}^{M-1} \tilde{H}_n(x_i)\tilde{H}_m(x_j) DHM_{n,m}(f). \tag{9}$$

Eq. (9) is in fact an inverse moment transformation. Stability of the inverse transformation is a very important indicator of the usefulness of the descriptors. Although the reconstruction itself is not the main goal (the main goal is a signal recognition by means of the descriptors), it illustrates and measures the recognition abilities of the descriptors. The possibility of a precise reconstruction is a proof that any two distinct signals can be discriminated. On the other hand, if the reconstruction is unstable, erroneous or even impossible, the recognition power of the descriptors is limited. The authors in Ref. [1] neither presented a reconstruction formula for their proposed THMs nor showed up any reconstruction experiment. We derived the formula analogous to Eq. (9) for THMs. However, since the kernel of their method includes two continuous polynomials $\{\overline{H}_n(x)\overline{H}_m(y)\}$ which are applied in a discrete double summation, the signal reconstruction from THMs is unstable, as we demonstrate in the next section.

4. Numerical experiments

4.1. Dynamic range of the moments

In the first experiment, we illustrate that the dynamic range of THMs is extremely high while that of DHMs is kept in a reasonably small interval. Due to this fact, we face precision loss of THMs in high values, which consequently contributes to wrong signal reconstruction.

We used two different discrete 1D signals with the same length of 60 samples. The range of amplitudes of these signals is $[0, 1]$ and $[0, 255]$, respectively, as is shown in Fig. 2(a) and (c). Fig. 2(b) and (d) compare the moment distribution for the proposed DHMs and THMs. In Fig. 2(b), the purple plot shows the values of the THMs of the first signal in the logarithmic scale and the red plot shows the values of the DHMs. It is clear from the graphs that the THMs are growing from 0 to extremely high values such as 10^{78} while the DHMs are bounded on $[-1, 1]$. If the input signal has been quantized into $[0, 255]$, the situation is similar – the THMs are growing to 10^{81} but the proposed DHMs are still within $[-250, 250]$ (see Fig. 2(d)).

For 2D signals, which we are mostly interested in, this effect is even more prominent. To illustrate that, we took a binary 16×16 image of capital E (see Fig. 3(a)) and computed its THMs and DHMs up to order 16. For the moment distributions, see Fig. 3(b) and (c).

4.2. Signal reconstruction

To show different reconstruction and recognition abilities of THMs and DHMs, we carried out the following experiments.

First, we used 1D signal from Fig. 2(a). We calculated DHMs up to order 60, which should theoretically provide a possibility of loss-less reconstruction. We reconstructed the original signal by means of Eq. (9) using various moment orders. Fig. 4(b)–4(i) illustrate the reconstructed signals if DHMs up to the order of 60, 59, 50, 40, 30, 20, 10 and 1, respectively, were used. For the order 60, the reconstruction is precise; for lower orders the precision slowly decreases.

Fig. 5 shows the same experiment using the THMs. It can be seen from Fig. 5(b) that even the complete set of THMs yields a totally wrong reconstruction due to the precision loss in moment computation.

In the second experiment, we performed the reconstruction test for the binary image of "E" as showed in Fig. 3(a). Table 1 illustrates the image reconstruction using the proposed DHMs. The maximum moment orders, used for the reconstruction, were from 1 to 16. In Table 1, we also present the reconstruction error for each moment order. Table 2 shows the same experiment using the THMs. As we can see, the reconstruction errors are much higher than in the case of DHMs and do not decrease if we increase the moment order, which contradicts the

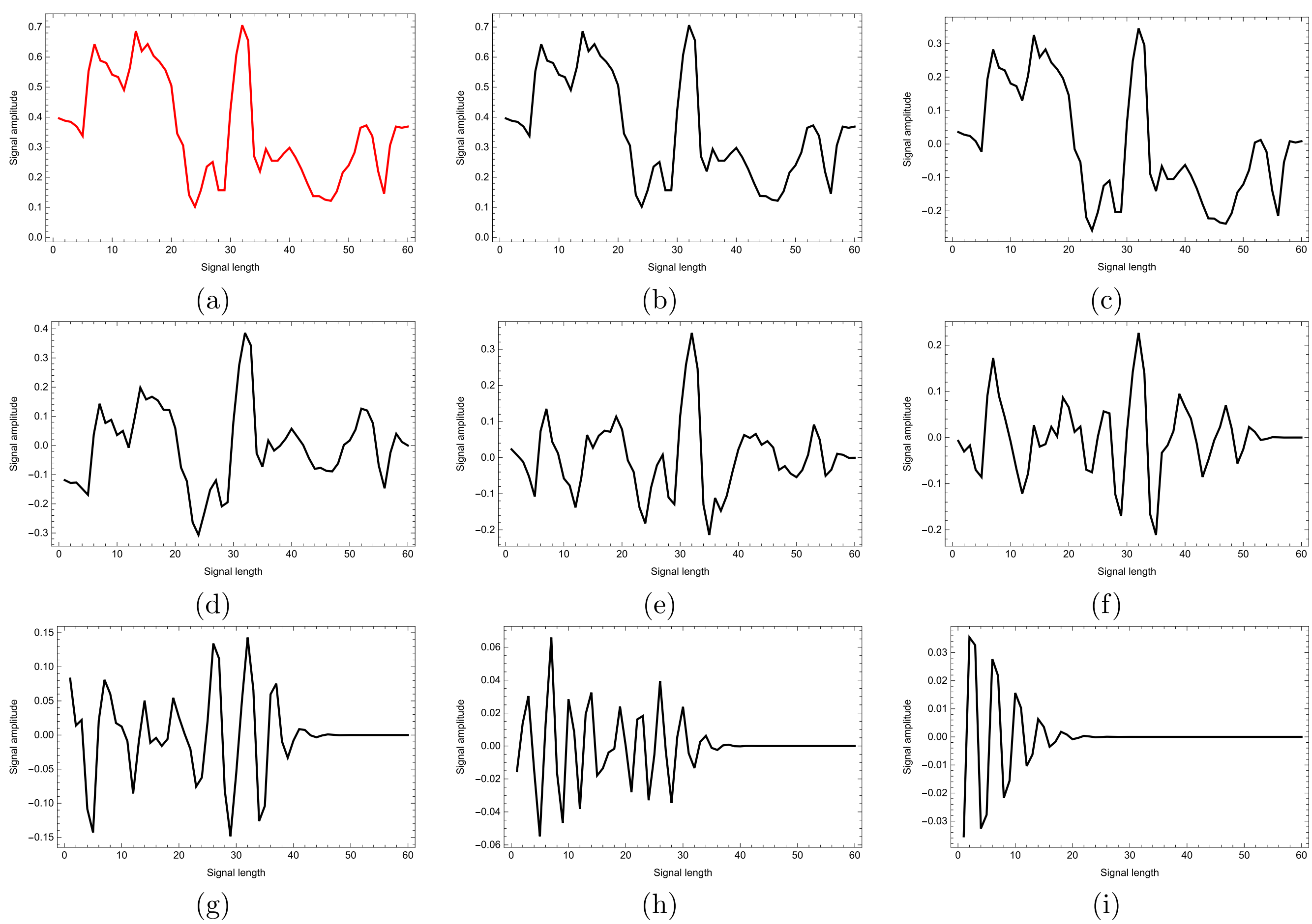

Fig. 4. 1D signal reconstruction using the DHMs with different maximum order of moments: (a) original signal, (b) reconstruction from DHMs up to the order 60, (c) order 59, (d) order 50, (e) order 40, (f) order 30, (g) order 20, (h) order 10 and (i) order 1.

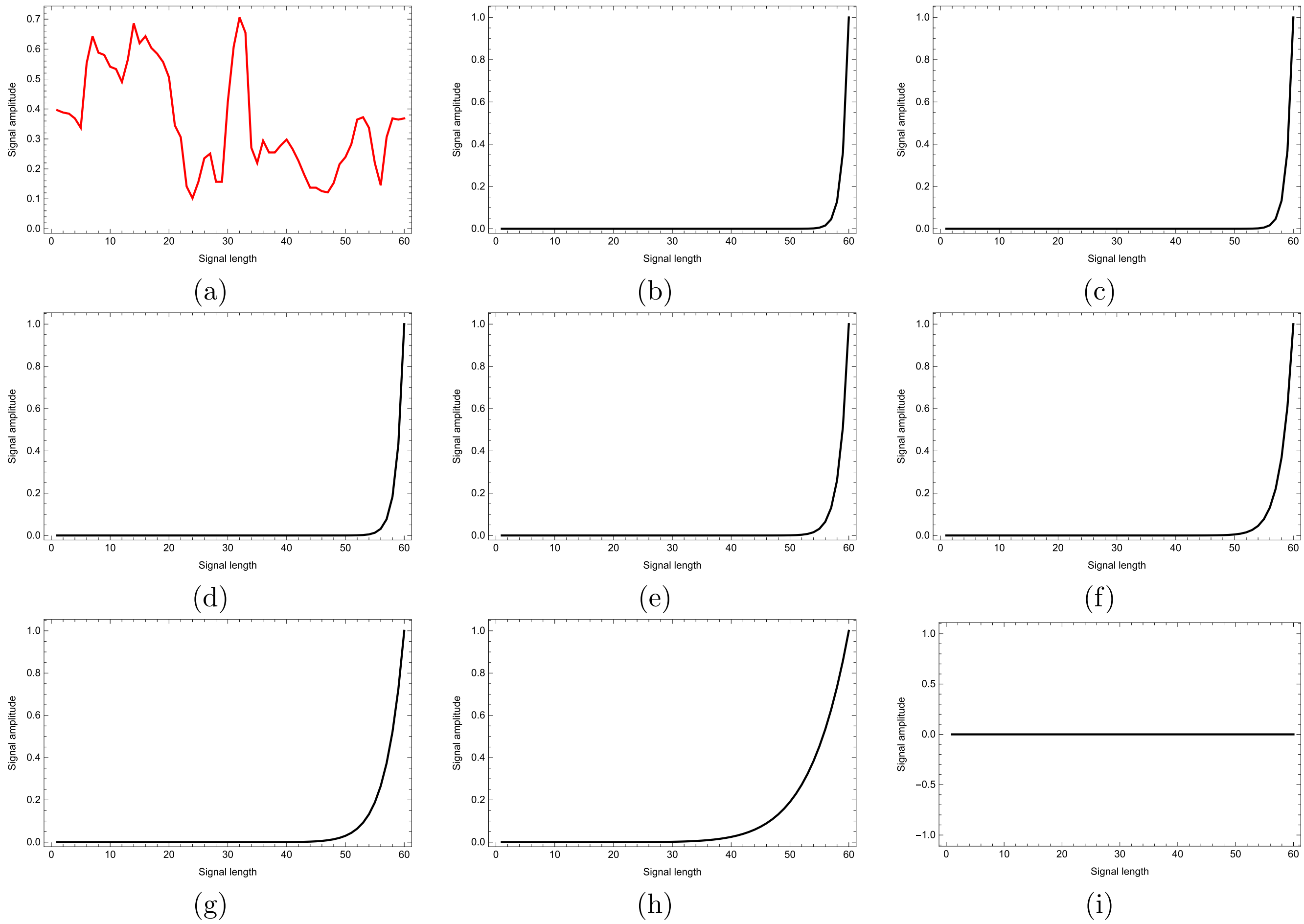

Fig. 5. 1D signal reconstruction using the THMs with different maximum order of moments: (a) original signal, (b) reconstruction from THMs up to the order 60, (c) order 59, (d) order 50, (e) order 40, (f) order 30, (g) order 20, (h) order 10 and (i) order 1.

Table 1
Image reconstruction of capital "E" of size 16 × 16 from orders 0 to 16 with their reconstruction errors using the proposed DHMs.

Original image				Rec.	image			
			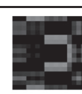			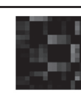		
Max. order	16	15	14	13	12	11	10	9
Recons. error	0.0000	0.9400	0.9435	0.9476	0.9520	0.9784	0.9820	0.9895
							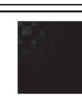	
Max. order	8	7	6	5	4	3	2	1
Recons. error	0.9901	0.9949	0.9963	0.9989	0.9991	0.9992	0.9997	0.9998

(continuous) theory.

5. Conclusion

The contribution of this paper is twofold. First, we pointed out and corrected the mathematical mistakes that appeared in Ref. [1]. We explained how Hermite polynomials should be applied in a discrete domain. Second, we demonstrated that the discrete orthogonality of the polynomials leads to much higher numerical precision than the approach proposed in Ref. [1]. Consequently, the proposed DHMs perform

Table 2
Image reconstruction of capital "E" of size 16 × 16 from orders 0 to 16 with their reconstruction errors using THMs.

Original image				Rec.	image			
								
Max. order	16	15	14	13	12	11	10	9
Recons. error	0.9890	0.9879	0.9867	0.9852	0.9834	0.9812	0.9785	0.9751
						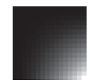	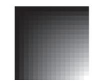	
Max. order	8	7	6	5	4	3	2	1
Recons. error	0.9706	0.9646	0.9561	0.9435	0.9231	0.8868	0.8167	1.0000

incomparably better than the THMs from Ref. [1] in signal/image reconstruction and recognition.

Acknowledgment

Barmak Honarvar has been financially supported by the Czech Science Foundation under the Grant No. 18-26018Y. Jan Flusser has been financially supported by the Czech Science Foundation under the Grant No. 18-07247S. Jan Flusser thanks the Joint Laboratory SALOME 2 for non-financial support.

References

[1] B.Q. Li, S.H. Lu, X. Wang, M.L. Xu, H.L. Zhai, Tchebichef–Hermite image moment method: a novel tool for chemometric analysis of three-dimensional spectra, Chemometr. Intell. Lab. Syst. 167 (Supplement C) (2017) 36–43.
[2] R. Mukundan, S. Ong, P.A. Lee, Image analysis by Tchebichef moments, IEEE Trans. Image Process. 10 (9) (2001) 1357–1364.
[3] J. Flusser, T. Suk, B. Zitová, 2D and 3D Image Analysis by Moments, John Wiley & Sons, 2016.
[4] B. Yang, M. Dai, Image reconstruction from continuous Gaussian–Hermite moments implemented by discrete algorithm, Pattern Recogn. 45 (4) (2012) 1602–1616.